RESEARCH ARTICLE



Check for updates

The role of atmospheric fronts in austral winter precipitation changes across Australia

Lindsay Lawrence¹ - 1

Rhys Parfitt¹ | Caroline C. Ummenhofer^{2,3}

¹Department of Earth, Ocean, and Atmospheric Science, Florida State University, Tallahassee, Florida, USA

²Department of Physical Oceanography, Woods Hole Oceanographic Institution, Woods Hole, Massachusetts, USA

³ARC Centre of Excellence for Climate Extremes, University of New South Wales, Sydney, New South Wales, Australia

Correspondence

Lindsay Lawrence, Department of Earth, Ocean, and Atmospheric Science, Florida State University, Tallahassee, Florida, USA.

Email: lml19g@my.fsu.edu

Funding information

James E. and Barbara V. Moltz Fellowship for Climate-Related Research at WHOI: National Science Foundation Division of Ocean Science, Grant/Award Number: 2023585

Abstract

Over the past few decades, Southeast Australia has experienced severe regional climatic events and some of the most extreme droughts on record, linked in part to influences from both the El Niño Southern Oscillation (ENSO) and the Indian Ocean Dipole (IOD). In this article, the extent to which austral winter rainfall anomalies, in years leading into co-occurring ENSO and IOD events, are communicated specifically through variations in atmospheric fronts is quantified. The most extreme wet (dry) conditions occur in winters characterized by sea surface temperature anomaly patterns exhibiting features of La Niña-Negative IOD (El Niño-Positive IOD). It is found that most of these precipitation anomalies are related to changes in the precipitation associated with the passing of atmospheric fronts specifically. Although there is some suggestion that there are accompanying changes in the frequency of atmospheric fronts, the response appears to be dominated by changes in the amount of precipitation per individual atmospheric front. In addition, the distribution in the dynamic strength of individual atmospheric fronts remains relatively unchanged.

KEYWORDS

atmospheric fronts, Australia, ENSO, extreme climate, IOD, precipitation

1 INTRODUCTION

In recent years, Australia has directly experienced the devastating effects of extreme climate events like flooding, drought, and bushfires. Of the \$18.2 billion in damages due to natural disasters from 2007 to 2016, approximately 47% of the cost of those disasters nation-wide have been attributed to either flood or bushfire events (Deloitte Access Economics, 2017). The eastern and southeastern portions of the country in particular are extremely vulnerable to these consequences of severe climate variability due to the high population densities. Many of these critical events are thought to be driven by oceanic variability, and traditionally have been linked to changes in the El Niño-Southern Oscillation (ENSO) (Nicholls et al., 1996; Reason et al., 2000; Suppiah, 2004). More recently however, studies have instead highlighted the first order role of the Indian Ocean Dipole (IOD), the second leading mode of monthly sea surface temperature (SST) variability in the Indian Ocean, and the leading mode in the austral cool season specifically (Black et al., 2021; Cai et al., 2009; Meyers et al., 2007; Min et al., 2013; Ummenhofer et al., 2009, 2011). Like ENSO, the IOD is partnered with anomalous large-scale atmospheric circulations and convective variations that force Rossby wave trains across the continent, propagating from the tropics to the extra-tropics,

This is an open access article under the terms of the Creative Commons Attribution License, which permits use, distribution and reproduction in any medium, provided the original work is properly cited.

© 2022 The Authors. Atmospheric Science Letters published by John Wiley & Sons Ltd on behalf of Royal Meteorological Society.

inducing climate variations across Australia and the southern hemisphere midlatitudes (Ashok et al., 2007; McIntosh & Hendon, 2018). Furthermore, the co-occurrence of certain phases of these climate modes have been shown to amplify the influence that each mode individually has on Australian meteorological extremes (Cai et al., 2011; Rathore et al., 2020; Ummenhofer et al., 2011).

In the Southern Hemisphere midlatitudes, much of the day-to-day precipitation variability is associated with atmospheric fronts. Despite the midlatitude storm track regions having the highest frontal frequency, the poleward portions of continents often exhibit localized frontal frequency maxima that are collocated with maxima in surface frontogenesis (Berry et al., 2011; Parfitt, Czaja, & Kwon, 2017; Parfitt, Czaja, & Seo, 2017; Satyamurty & Fernado De Mattos, 1989). In winter months especially, a belt of high frontal frequency can extend further into the subtropical latitudes, and precipitation associated with those fronts can also be displaced beyond the extent of the identified frontal grid point (Papritz et al., 2014). Across eastern and southern Australia, it has been shown that a large fraction of the annual precipitation is associated with the passing of these atmospheric fronts (Catto et al., 2012; Pepler et al., 2020; Soster & Parfitt, 2021), although this fraction exhibits significant seasonal variability and is generally lowest in wintertime. While studies have shown that El Niño (La Niña) is associated with a midlatitude atmospheric frontal frequency reduction (increase) in the South Pacific during the June, July, and August (JJA) season (Rudeva & Simmonds, 2015), the influence of the IOD on atmospheric fronts has yet to be addressed. It is also noted that Rudeva and Simmonds (2015) illustrated that atmospheric fronts tend to explain more variance in Southern Hemisphere climate than extratropical cyclones. As such, this article seeks to address the influence of atmospheric fronts on precipitation across Australia in the austral winter leading into co-occurring ENSO and IOD events. In particular:

- 1. How much anomalous precipitation during winters leading into co-occurring ENSO and IOD events in Australia is frontal?
- 2. Of the precipitation that is frontal, how extreme are such events?
- 3. What frontal characteristics are responsible for the changes in frontal precipitation over Australia?

2 | DATA AND METHODS

In this study, we use 6-hourly data from the European Centre for Medium-Range Weather Forecasts (ECMWF) 5th Generation Reanalysis (ERA5) (Hersbach et al., 2020) for the period 1979–2018. ERA5 has a global horizontal resolution of $0.25^{\circ} \times 0.25^{\circ}$ (\sim 31 km).

In order to understand the role that atmospheric fronts play in Australian climate, we implement an objective frontal diagnostic, the "F-diagnostic" (Parfitt, Czaja, & Kwon, 2017; Parfitt, Czaja, & Seo, 2017). The Fdiagnostic is given by the variable $F = \frac{\zeta_p |\nabla T_p|}{f |\nabla T|_p}$, where ζ_p is the isobaric relative vorticity, ∇T_p is the isobaric temperature gradient, f is the Coriolis parameter, and $|\nabla T|_{a}$ is a temperature gradient typical (taken to $4.5 \times 10^{-3} \text{K km}^{-1}$ at 900 hPa). Surface fronts are identified at 900 hPa as recommended by Hewson (1998), and frontal grid points are identified where >1, with the additional criteria that frontal grid points must have a contiguous extension of at least 500 km to be identified as an atmospheric front. For any identified atmospheric front, a measure of the frontal strength is defined simply as the normalized value of the F-diagnostic. Meanwhile, precipitation is assigned to an atmospheric front based on the proximity to a $5^{\circ} \times 5^{\circ}$ search box centered on the precipitation, following the methodology of both Catto et al. (2012) and Soster and Parfitt (2021). It is noted here that while multiple objective frontal diagnostics exist (e.g., Hewson, 1998; Simmonds et al., 2012), each with their own strengths (e.g., Hope et al., 2014; Schemm et al., 2015; Thomas & Schultz, 2019 for further discussion) the F-diagnostic is chosen, as this combination of the specific quantities has been shown to aid in the identification of the associated frontal rainband (Solman & Orlanski, 2014). An example of a frontal rainband propagating across Australia, at 0000UTC on 8 August 1999, is shown in Figure S1a, with the associated atmospheric fronts plotted using the F-diagnostic. It is noted that the identification of occasional small-scale frontal features in the sub-tropics is common across objective frontal identification methods, particularly when identified in higherresolution datasets such as ERA-5 (Soster & Parfitt, 2021). For reference, in Figure S1b, the same figure is also reproduced using the objective diagnostic of Hewson (1998), termed here the "T-diagnostic".

To evaluate how ENSO and IOD impact the behavior of atmospheric fronts and frontal precipitation, we use the classification indices calculated by Rathore et al. (2020) for 1979–2016, and extended further using the same methodology for 2017 and 2018. This classification uses the Niño-3.4 index for the November–February seasonally averaged time series to define ENSO years and the August–November seasonally averaged time series to define the dipole mode index (DMI) for the IOD years, to categorize each year as Pure El Niño (EN), Pure La Niña (LN), Pure Positive IOD (pIOD), Pure Negative IOD (nIOD), co-occurring El Niño and Positive IOD (EN-pIOD), and co-occurring La Niña and Negative

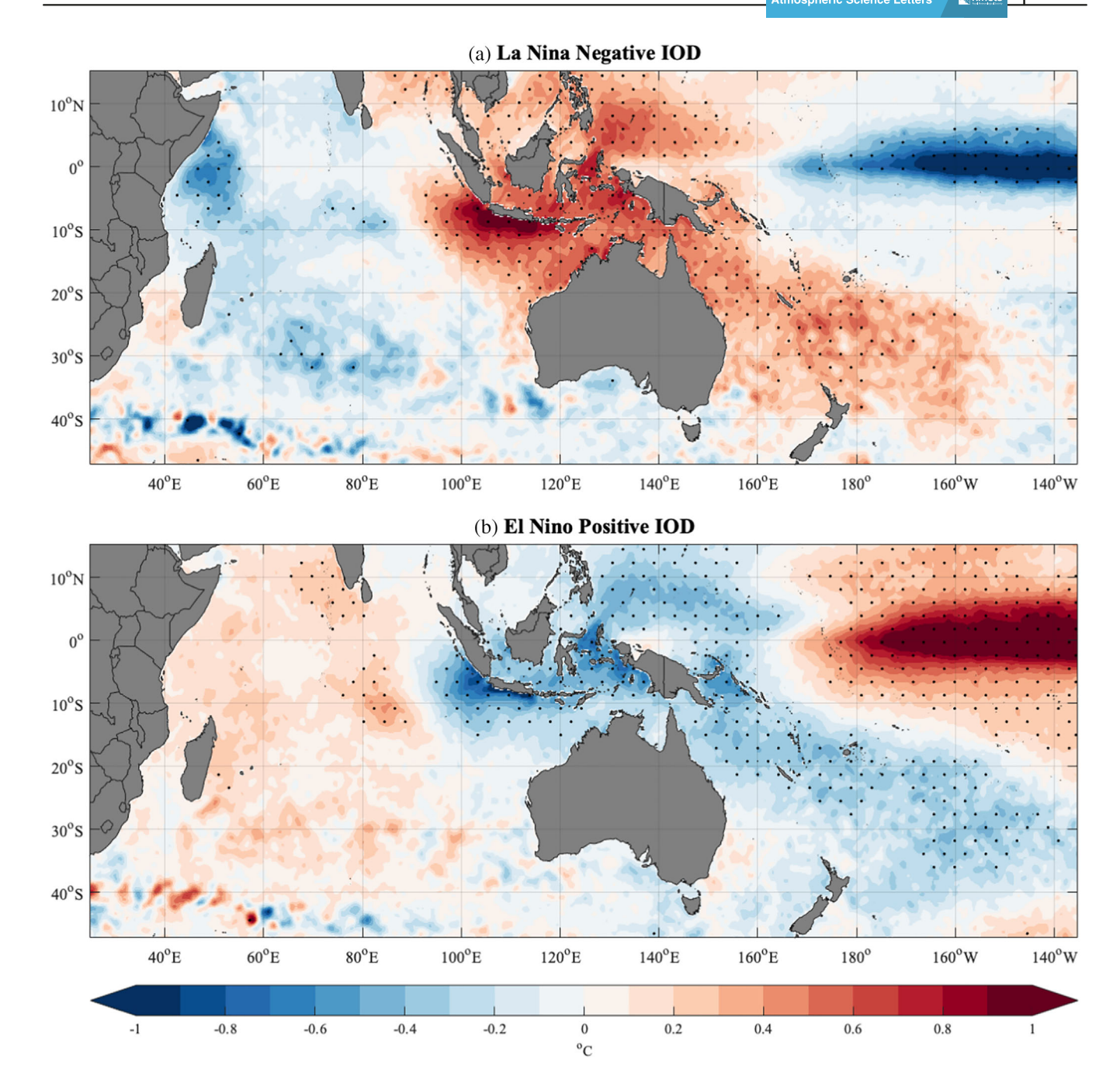


FIGURE 1 (a) JJA SST anomalies leading into La Niña-nIOD events relative to 1979–2018 JJA climatology, with stippling indicating anomalies significant at 90% via a two-tailed Student's *t* test. (b) As in as (a), but for El Niño-pIOD.

IOD (LN-nIOD) (see Table S1). It is noted that although the focus of the analyses is on the JJA season for those years leading *into* the months chosen to define ENSO years above, the difference with regards to the SST anomalies identified in the JJA season (Figure 1) are virtually indistinguishable from those identified when austral cool season months are used to define ENSO years (c.f. Figure 2 from Ummenhofer et al., 2011). We choose to define the indices as above to allow a more direct comparison with recent studies such as Rathore

et al. (2020). All data is detrended prior to composite analysis below.

3 | RESULTS

Figure 2a,d illustrate the anomalous JJA monthly precipitation rate leading into LN-nIOD and EN-pIOD events, respectively. A significant increase (decrease) in the amount of moisture transported over the Australian

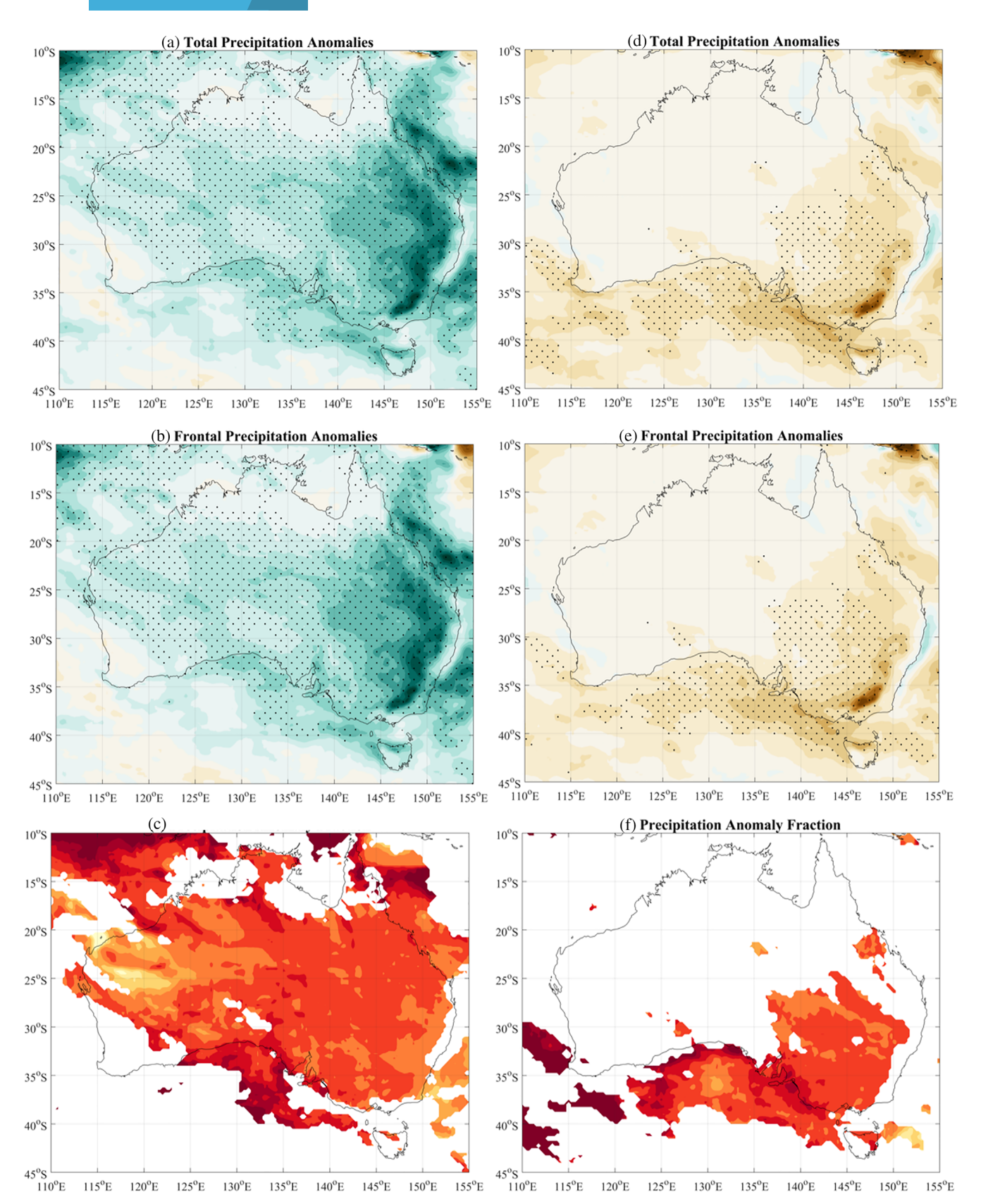


FIGURE 2 (a) Total JJA precipitation anomalies leading into La Niña-nIOD events relative to 1979–2018 JJA climatology, with stippling indicating anomalies significant at 90% via a two-tailed Student's *t* test. (b) As in (a) but for frontal precipitation anomalies. (c) The ratio of JJA frontal precipitation anomalies to JJA total precipitation anomalies leading into La Niña-nIOD events, given as a percentage, for areas where total precipitation anomalies are significant to 90%. (d–f) As in (a–c), but for El Niño-pIOD.

5 of 9

continent occurs during winters leading into co-occurring negative (positive) IOD events with La Niña (El Niño), with maxima predominantly seen in the eastern and southern regions of Australia. Conversely, the anomalies associated with other classifications of ENSO and IOD are relatively muted in comparison (Figure S2). As such, we choose to focus here on the LN-nIOD and EN-pIOD classifications specifically.

Figure 2b, e illustrate analogous composites for the frontal precipitation. Comparison with Figure 2a,d immediately reveals an extremely high degree of similarity. This suggests that most of the JJA precipitation anomalies across Australia in winters leading into co-occurring LN-nIOD and EN-pIOD conditions are associated with changes to the precipitation accompanying passing atmospheric fronts. This is quantified in Figure 2c,f, which show the percentage of the precipitation anomalies associated with LN-nIOD and EN-pIOD events, respectively, that results from frontal precipitation—across most of the Australian continent, this percentage exceeds 90%. In other words, of the total precipitation anomalies in east and southeast Australia seen during winters characterized by developing LN-nIOD and EN-pIOD conditions, over 90% of the anomaly pattern can be attributed to changes in anomalous frontal precipitation. It is noted that in several locations to the south of Australia, this percentage is actually slightly >100%, indicative of potentially significant changes to types of rainfall that are nonfrontal.

Having shown that anomalous precipitation in austral winters leading into LN-nIOD and EN-pIOD is primarily associated with the passing of an atmospheric front, the next issue to consider is how the characteristics of those atmospheric fronts and their associated rainfall vary in those areas with statistically significant anomalies in Figure 2. For example, changes to the dynamic strength of the passing atmospheric fronts may indicate a strengthening mechanism (e.g., Parfitt et al., 2016) associated with IOD-induced SST temperature gradient changes.

Figure 3a,b shows that during JJA months leading into LN-nIOD (EN-pIOD), there is an increase (decrease) in atmospheric frontal frequency over much of the northern Australian continent. During JJA months leading into LN-nIOD, there are also increases across centraleastern Australia as well. It is noted that the anomalous values given are absolute—that is, a value of 0.05 would indicate that atmospheric fronts are present on 5% more of the total wintertime days (as opposed to a 5% increase in the number of fronts). Comparison with a JJA frontal climatology (Figure S3) illustrates that these absolute values represent percentage changes in frontal frequency of up to \sim 30%. This suggests that some of the anomalous frontal precipitation associated with the LN-nIOD and

EN-pIOD events might be occurring due to a corresponding increase in the frequency of atmospheric fronts propagating across the Australian continent. It is noted that one does not necessarily expect the anomalous frontal frequency to match exactly the areas of anomalous precipitation, due to frontal precipitation often extending beyond the grid points deemed to be frontal. There are other factors however that could be contributing to this change, such as fluctuations in the dynamic strength of individual atmospheric fronts, as well as variability in the amount of rainfall per individual atmospheric front.

To address this, the probability density functions (PDFs) of both the frontal precipitation rate and atmospheric frontal strength, taken as the magnitude of the Fdiagnostic, are plotted in Figure 3c,d, respectively, for Coolabah, New South Wales, where there are statistically significant changes in frontal frequency for both LNnIOD and EN-pIOD events. The corresponding distributions for all JJA months are also plotted in each figure. We can see that the distributions in the frontal strength leading into both the LN-nIOD and EN-pIOD events are relatively unchanged from average conditions. This suggests that any identified change in frontal frequency is distributed equally across all frontal strengths. The lack of obvious change in the distribution of JJA frontal strength during austral winters leading into LN-nIOD and EN-pIOD suggests that the frontal frequency anomalies in Coolabah are likely not a result of direct strengthening of atmospheric fronts via surface temperature gradient changes, but rather a shift in the track of atmospheric fronts. Indeed, it has been previously noted that SST anomalies influence thickness gradients, which in turn alters thermal wind patterns and the subsequent potential for the formation of midlatitude frontal systems in Australia (Risbey et al., 2009). Furthermore, Rudeva et al. (2019) also highlighted to first order that significant correlations exist between the number of fronts in the low midlatitudes and the location and intensity of the subtropical ridge, and an equatorward-shifted southern hemisphere wintertime subtropical jet has also been shown to be eddy driven and associated with the poleward displacement of the eddy-driven jet (Gillett et al., 2021). In addition, Parfitt and Kwon (2020) demonstrated that the trajectory of atmospheric fronts covaries with the latitude of the eddy-driven jet.

Analysis of the frontal precipitation distributions however indicates that moderate to intense frontal precipitation rates occur much more (less) frequently for LN-nIOD (EN-pIOD) events (with very little change in low frontal precipitation values in either phase). This suggests that the anomalous JJA frontal precipitation occurring leading into LN-nIOD and EN-pIOD events in

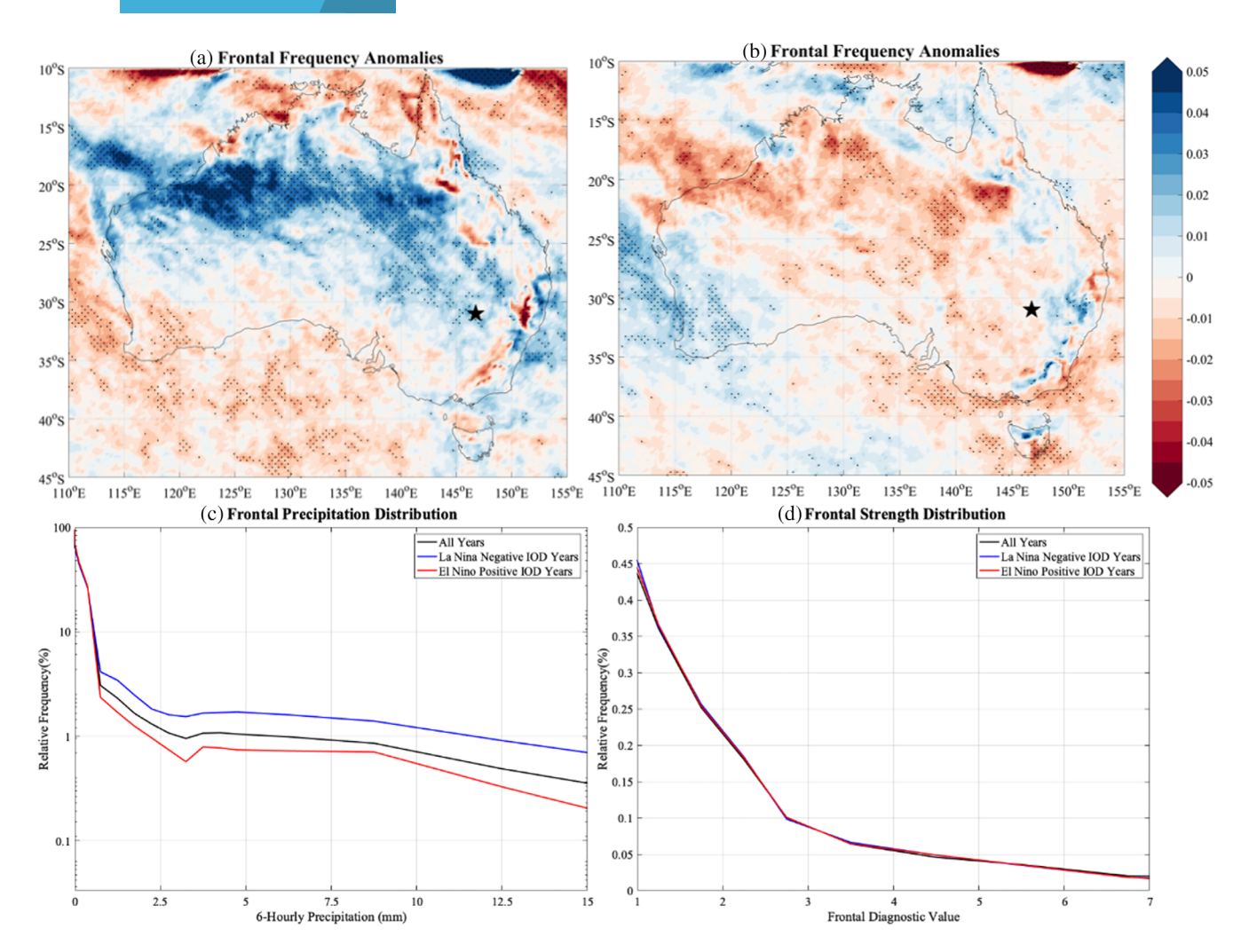


FIGURE 3 (a) Absolute JJA anomalies in frontal frequency relative to 1979–2018 JJA climatology leading into La Niña-nIOD events with stippling indicating anomalies significant at 90% via a two-tailed Student's *t* test. (b) As in (a) but for El Niño-pIOD. (c) Probability density function taken in Coolabah, NSW, marked as a star, of the frontal precipitation rate during all winters in the JJA climatology as compared to those leading into La Niña-nIOD (blue) and El Niño-pIOD (red) events. (c) As in (b), but for the frontal strength during all winters in the JJA climatology as compared to those leading into the La Niña-nIOD (blue) and El Niño-pIOD (red) events.

Coolabah is heavily influenced by changes in the amount of precipitation occurring during the strongest frontal precipitation events. The lack of change in the frontal strength distributions further suggests that these changes in precipitation rates in Coolabah are likely driven by anomalous moisture availability, consistent with the findings in Rathore et al. (2020). Nevertheless, it is noted that these varying precipitation rates across eastern and southeastern Australia may also be explained by changes to atmospheric conditions at pressure levels other than 900 hPa, or by factors simply not well-represented by the F-diagnostic. These analyses were performed at several other locations across the east and south of Australia (not shown), with the same conclusions. Combined with the fact that large regions of eastern and southeastern Australia show no statistically significant change in frontal frequency, it seems likely that the frontal precipitation

changes in those regions leading into LN-nIOD and EN-pIOD events are in fact dominated by the changes in the precipitation rate of individual atmospheric fronts. Furthermore, despite the limited sample size associated with the LN-nIOD and EN-pIOD classifications (six and nine events, respectively), analysis of the frontal rainfall in any individual season in our study consistently showed a very high degree of similarity with our composite averages, whereas similar analysis for the frontal frequency displayed a higher degree of noise (not shown).

Lastly however, it is noted that in the region characterized by the largest frontal frequency changes, northwest Australia, some changes to the frontal strength distribution leading into LN-nIOD and EN-pIOD events can be identified (see Figure S4 for an example in Pippingarra, Western Australia), with the weakest atmospheric fronts primarily affected. Furthermore, identified

7 of 9

changes in the precipitation per individual atmospheric front, while still notable, are significantly less so than for locations in eastern and southern Australia. Previous studies (Parfitt et al., 2016, Parfitt, Czaja, & Kwon, 2017; Parfitt, Czaja, & Seo, 2017) have suggested changes in surface temperature gradients (as would occur for example off the coast of Northwest Australia due to SST anomalies leading into a co-occurring LN-nIOD event, c.f. Figure 1) can significantly alter atmospheric frontogenesis through diabatic heating effects. Further studies by Masunaga et al. (2020) and Reeder et al. (2021) suggest that any such effect would likely manifest in changes to the very weakest, or quasi-stationary fronts, as is found here. As such, one possibility is that precipitation changes in Northwest Australia may be influenced by direct SST impacts on atmospheric frontal frequency. While this is beyond the scope of the present study, research is currently underway to fully investigate this possibility.

CONCLUSIONS

In this article, we addressed the relationship between precipitation changes in austral winters leading into cooccurring IOD and ENSO events, and atmospheric fronts (identified with the "F-diagnostic") in the ERA5 reanalysis dataset. Our results indicate that for winters leading into co-occurring negative (positive) IOD and La Niña (El Niño), the eastern and southeastern regions of Australia experience anomalously wet (dry) conditions. Of the anomalously wet (dry) wintertime conditions found leading into LN-nIOD (EN-pIOD) events, frontal precipitation anomalies account for almost all of the precipitation anomalies. It is further revealed that although the distribution in the strength of atmospheric fronts is unchanged during LN-nIOD (EN-pIOD), their frequency increases (decreases) across much of Australia. Furthermore, an increase (decrease) in extreme frontal precipitation rates is also observed during winters leading into LN-nIOD (EN-pIOD). It is concluded however that across eastern and southern Australia, it is likely the precipitation anomaly per front that dominates the contribution of atmospheric frontal changes to total precipitation changes. This is consistent with previously identified corresponding changes in moisture transport (Rathore et al., 2020), as well as changes to austral cool season frontal precipitation being dominated by changes in rainfall intensity (Pepler et al., 2021). While this conclusion is also generally true for northwest Australia specifically, our results suggest the potential of a larger role for frontal frequency anomalies in that region, although further work must be done to fully investigate the mechanistic

driver. It is noted that all analyses involving atmospheric fronts in this manuscript were also reproduced using a different objective frontal diagnostic (the "T-diagnostic"—Hewson, 1998), with the results remaining consistent (not shown). It is also emphasized that all of the aforementioned precipitation and atmospheric frontal anomalies identified during winters leading into LNnIOD and EN-pIOD events in this study were found to be asymmetric with respect to the co-occurrence of phases (i.e., LN-nIOD and EN-pIOD phases do not correspond to equal but opposite atmospheric responses). These conclusions further illustrate the central role that atmospheric fronts play in the influence of both ENSO and the IOD on Australian climate. Given the sensitivity of atmospheric frontal representation in reanalyses and models to horizontal resolution (Soster & Parfitt, 2021), a natural next step would also be to investigate the role of atmospheric fronts in contributing to inter-model biases regarding atmospheric impacts of ENSO and the IOD.

AUTHOR CONTRIBUTIONS

Lindsay Lawrence: Formal analysis; investigation; methodology; validation; visualization; writing - original draft; writing - review and editing. Rhys Parfitt: Conceptualization; funding acquisition; investigation; supervision; writing - review and editing. Caroline Ummenhofer: Conceptualization; funding acquisition; investigation; writing - review and editing.

ACKNOWLEDGMENTS

We would like to thank ECMWF for access to the ERA-5 dataset, and Frederick Soster for his assistance with the frontal data. Rhys Parfitt would like to gratefully acknowledge NSF OCE award number 2023585 and Caroline C. Ummenhofer support from the James E. and Barbara V. Moltz Fellowship for Climate-Related Research at WHOI.

ORCID

Lindsay Lawrence https://orcid.org/0000-0002-5161-

Rhys Parfitt https://orcid.org/0000-0002-2133-8057

REFERENCES

Ashok, K., Nakamura, H. & Yamagata, T. (2007) Impacts of ENSO and Indian Ocean dipole events on the southern hemisphere storm-track activity during austral winter. Journal of Climate, 20, 3147-3163. https://doi.org/10.1175/JCLI4155.1

Berry, G., Reeder, M.J. & Jakob, C. (2011) A global climatology of atmospheric fronts. Geophysical Research Letters, 38, L04809. https://doi.org/10.1029/2010GL046451

Black, A.S., Risbey, J.S., Chapman, C.C., Monselesan, D.P., Moore, T.S., Pook, M.J. et al. (2021) Australian northwest Cloudbands and their relationship to atmospheric Rivers and

- precipitation. *Monthly Weather Review*, 149(4), 1125–1139. https://doi.org/10.1175/mwr-d-20-0308.1
- Cai, W., Cowan, T. & Raupach, M. (2009) Positive Indian Ocean dipole events precondition Southeast Australia bushfires. Geophysical Research Letters, 36, L19710. https://doi.org/10.1029/ 2009GL039902
- Cai, W., van Rensch, P., Cowan, T. & Hendon, H.H. (2011) Teleconnection pathways of ENSO and the IOD and the mechanisms for impacts on Australian rainfall. *Journal of Climate*, 24(15), 3910–3923. https://doi.org/10.1175/2011JCLI4129.1
- Catto, J.L., Jakob, C., Berry, G. & Nicholls, N. (2012) Relating global precipitation to atmospheric fronts. *Geophysical Research Let*ters, 39(10), 1–6. https://doi.org/10.1029/2012GL051736
- Deloitte Access Economics. (2017) Building resilience to natural disasters in our states and territories. Sydney: New South Wales.
- Gillett, Z.E., Hendon, H.H., Arblaster, J.M. & Lim, E.P. (2021) Tropical and extratropical influences on the variability of the southern hemisphere wintertime subtropical jet. *Journal of Climate*, 34(10), 4009–4022. https://doi.org/10.1175/JCLI-D-20-0460.1
- Hersbach, H., Bell, B., Berrisford, P., Hirahara, S., Horányi, A., Muñoz-Sabater, J. et al. (2020) The ERA5 global reanalysis. Quarterly Journal of the Royal Meteorological Society, 146(730), 1999–2049. https://doi.org/10.1002/QJ.3803
- Hewson, T.D. (1998) Objective fronts. *Meteorological Applications*, 5(1), 37–65. https://doi.org/10.1017/S1350482798000553
- Hope, P., Keay, K., Pook, M., Catto, J., Simmonds, I., Mills, G. et al. (2014) A comparison of automated methods of front recognition for climate studies: a case study in southwest Western Australia. *Monthly Weather Review*, 142(1), 343–363. https://doi.org/10.1175/MWR-D-12-00252.1
- Masunaga, R., Nakamura, H., Taguchi, B. & Miyasaka, T. (2020) Processes shaping the frontal-scale time-mean surface wind convergence patterns around the Kuroshio extension in winter. *Journal of Climate*, 33(1), 3–25. https://doi.org/10.1175/JCLI-D-19-0097.1
- McIntosh, P.C. & Hendon, H.H. (2018) Understanding Rossby wave trains forced by the Indian Ocean dipole. *Climate Dynamics*, 50(7–8), 2783–2798. https://doi.org/10.1007/s00382-017-3771-1
- Meyers, G., McIntosh, P., Pigot, L. & Pook, M. (2007) The years of El Niño, La Niña and interactions with the tropical Indian Ocean. *Journal of Climate*, 20(13), 2872–2880. https://doi.org/10.1175/JCLI4152.1
- Min, S.K., Cai, W. & Whetton, P. (2013) Influence of climate variability on seasonal extremes over Australia. *Journal of Geophysical Research Atmospheres*, 118(2), 643–654. https://doi.org/10.1002/jgrd.50164
- Nicholls, N., Lavery, B., Frederiksen, C., Drosdowsky, W. & Torok, S. (1996) Recent apparent changes in relationships between the El Niño: Southern oscillation and Australian rainfall and temperature. *Geophysical Research Letters*, 23(23), 3357–3360.
- Papritz, L., Pfahl, S., Rudeva, I., Simmonds, I., Sodemann, H. & Wernli, H. (2014) The role of extratropical cyclones and fronts for Southern Ocean freshwater fluxes. *Journal of Climate*, 27(16), 6205–6224. https://doi.org/10.1175/JCLI-D-13-00409.1
- Parfitt, R., Czaja, A. & Kwon, Y.-O. (2017) The impact of SST resolution change in the ERA-interim reanalysis on wintertime gulf stream frontal air-sea interaction. *Geophysical Research Letters*, 44, 3246–3254. https://doi.org/10.1002/2017GL073028

- Parfitt, R., Czaja, A., Minobe, S. & Kuwano-Yoshida, A. (2016) The atmospheric frontal response to SST perturbations in the Gulf stream region. *Geophysical Research Letters*, 43(5), 2299–2306. https://doi.org/10.1002/2016GL067723
- Parfitt, R., Czaja, A. & Seo, H. (2017) A simple diagnostic for the detection of atmospheric fronts. *Geophysical Research Letters*, 44(9), 4351–4358. https://doi.org/10.1002/2017GL073662
- Parfitt, R. & Kwon, Y.O. (2020) The modulation of gulf stream influence on the troposphere by the eddy-driven jet. *Journal of Climate*, 33(10), 4109–4120. https://doi.org/10.1175/JCLI-D-19-0294.1
- Pepler, A.S., Dowdy, A.J. & Hope, P. (2021) The differing role of weather systems in southern Australian rainfall between 1979–1996 and 1997–2015. *Climate Dynamics*, 56(7), 2289–2302. https://doi.org/10.1007/s00382-020-05588-6
- Pepler, A.S., Dowdy, A.J., van Rensch, P., Rudeva, I., Catto, J.L. & Hope, P. (2020) The contributions of fronts, lows and thunder-storms to southern Australian rainfall. *Climate Dynamics*, 55(5), 1489–1505. https://doi.org/10.1007/s00382-020-05338-8
- Rathore, S., Bindoff, N.L., Ummenhofer, C.C., Phillips, H.E. & Feng, M. (2020) Near-surface salinity reveals the oceanic sources of moisture for australian precipitation through atmospheric moisture transport. *Journal of Climate*, 33(15), 6707–6730. https://doi.org/10.1175/JCLI-D-19-0579.1
- Reason, C.J.C., Allan, R.J., Lindesay, J.A. & Ansell, T.J. (2000) Enso and climatic signals across the Indian Ocean basin in the global context: part I, interannual composite patterns. *International Journal of Climatology*, 20(11), 1285–1327. https://doi.org/10.1002/1097-0088(200009)20:11<1285::AID-JOC536>3.0.CO;2-R
- Reeder, M.J., Spengler, T. & Spensberger, C. (2021) The effect of sea surface temperature fronts on atmospheric frontogenesis. *Jour*nal of the Atmospheric Sciences, 78(6), 1753–1771. https://doi. org/10.1175/JAS-D-20-0118.1
- Risbey, J.S., Pook, M.J., McIntosh, P.C., Ummenhofer, C.C. & Meyers, G. (2009) Characteristics and variability of synoptic features associated with cool season rainfall in southeastern Australia. *International Journal of Climatology*, 29, 1595–1613. https://doi.org/10.1002/joc.1775
- Rudeva, I. & Simmonds, I. (2015) Variability and trends of global atmospheric frontal activity and links with large-scale modes of variability. *Journal of Climate*, 28(8), 3311–3330. https://doi.org/10.1175/JCLI-D-14-00458.1
- Rudeva, I., Simmonds, I., Crock, D. & Boschat, G. (2019) Midlatitude fronts and variability in the southern hemisphere tropical width. *Journal of Climate*, 32(23), 8243–8260. https://doi.org/10.1175/JCLI-D-18-0782.1
- Satyamurty, P. & Fernado De Mattos, L. (1989) Climatological lower tropospheric frontogenesis in the Midlatitudes due to horizontal deformation and divergence. *Monthly Weather Review*, 117(6), 1355–1364. https://journals.ametsoc.org/view/journals/mwre/117/6/1520-0493_1989_117_1355_cltfit_2_0_co_2.xml
- Schemm, S., Rudeva, I. & Simmonds, I. (2015) Extratropical fronts in the lower troposphere–global perspectives obtained from two automated methods. *Quarterly Journal of the Royal Meteorological Society*, 141(690), 1686–1698. https://doi.org/10.1002/QJ.2471
- Simmonds, I., Keay, K. & Bye, J.A.T. (2012) Identification and climatology of southern hemisphere mobile fronts in a modern reanalysis. *Journal of Climate*, 25(6), 1945–1962. https://doi.org/10.1175/JCLI-D-11-00100.1

9 of 9

- Solman, S.A. & Orlanski, I. (2014) Poleward shift and change of frontal activity in the southern hemisphere over the last 40 years. Journal of the Atmospheric Sciences, 71(2), 539-552. https://doi.org/10.1175/JAS-D-13-0105.1
- Soster, F. & Parfitt, R. (2022). On objective identification of atmospheric fronts and frontal precipitation in reanalysis datasets. Journal of Climate, 35(14), 4513-4534. https://doi.org/10.1175/ JCLI-D-21-0596.1
- Suppiah, R. (2004) Trends in the southern oscillation phenomenon and Australian rainfall and changes in their relationship. International Journal of Climatology, 24(3), 269-290. https://doi.org/ 10.1002/JOC.1001
- Thomas, C.M. & Schultz, D.M. (2019) What are the best thermodynamic quantity and function to define a front in gridded model output? Bulletin of the American Meteorological Society, 100(5), 873-895. https://doi.org/10.1175/BAMS-D-18-0137.1
- Ummenhofer, C.C., England, M.H., McIntosh, P.C., Meyers, G.A., Pook, M.J., Risbey, J.S. et al. (2009) What causes Southeast Australia's worst droughts? Geophysical Research Letters, 36, L04706. https://doi.org/10.1029/2008GL036801

Ummenhofer, C.C., Sen Gupta, A., Briggs, P.R., England, M.H., McIntosh, P.C., Meyers, G.A. et al. (2011) Indian and Pacific Ocean influences on southeast Australian drought and soil moisture. Journal of Climate, 24(5), 1313-1336. https://doi.org/ 10.1175/2010JCLI3475.1

SUPPORTING INFORMATION

Additional supporting information can be found online in the Supporting Information section at the end of this article.

How to cite this article: Lawrence, L., Parfitt, R., & Ummenhofer, C. C. (2022). The role of atmospheric fronts in austral winter precipitation changes across Australia. Atmospheric Science Letters, e1117. https://doi.org/10.1002/asl.1117